Parallel Adaptive Cartesian Upwind Methods for Shock-Driven Multiphysics Simulation

Ralf Deiterding

Computer Science and Mathematics Division
Oak Ridge National Laboratory
P.O. Box 2008 MS6367, Oak Ridge, TN 37831, USA
E-mail: deiterdingr@ornl.gov

33th Brazilian National Congress on Applied and Computational Mathematics
September 22, 2010

Collaboration with

- Sean Mauch and Daniel Meiron (Computational and Applied Mathematics, California Institute of Technology)
- Fehmi Cirak (Mechanical Engineering, University of Cambridge)
- Stuart Laurence (Institut for Aeroelastic, DLR Göttingen)
- Joseph Shepherd, Hans Hornung (Graduate Aeronautical Laboratories, Caltech)
- Georg Bader (Institut for Mathematics, Technical University Cottbus)

This work was sponsored by the Office of Advanced Scientific Computing Research; U.S. Department of Energy (DOE) and was performed at the Oak Ridge National Laboratory, which is managed by UT-Battelle, LLC under Contract No. DE-AC05-00OR22725. Part of this work was performed at the California Institute of Technology and was supported by the ASC program of the Department of Energy under subcontract No. B341492 of DOE contract W-7405-ENG-48. Part of this work was also performed at the Technical University Cottbus, Germany and was supported by the German Science Foundation, grant Ba 840/3-3.

Outline

Outline

Hyperbolic Conservation Laws

$$\partial_t \mathbf{q}(\mathbf{x},t) + \nabla \cdot \mathbf{f}(\mathbf{q}(\mathbf{x},t)) = \mathbf{s}(\mathbf{q}(\mathbf{x},t))$$

Integral form (Gauss's theorem):

$$\int_\Omega \mathbf{q}(\mathbf{x}, t+\Delta t)\, d\mathbf{x} - \int_\Omega \mathbf{q}(\mathbf{x}, t)\, d\mathbf{x}$$

$$+ \int_t^{t+\Delta t} \int_{\partial\Omega} \mathbf{f}(\mathbf{q}(\mathbf{o},t))\,\sigma(\mathbf{o})\, d\mathbf{o}\, dt = \int_t^{t+\Delta t} \int_\Omega \mathbf{s}(\mathbf{q}(\mathbf{x},t))\, d\mathbf{x}$$

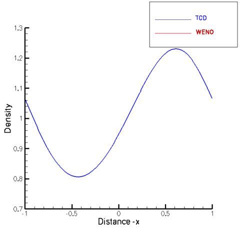

Example: Euler equations

Time discretization $t_n = n\Delta t$, discrete volumes $I_j = [x_j - \frac{1}{2}\Delta x, x_j + \frac{1}{2}\Delta x[=: [x_{j-1/2}, x_{j+1/2}[$

Using approximations $\mathbf{Q}_j(t) \approx \frac{1}{|I_j|}\int_{I_j} \mathbf{q}(\mathbf{x},t)\, dx$, $\quad \mathbf{s}(\mathbf{Q}_j(t)) \approx \frac{1}{|I_j|}\int_{I_j} \mathbf{s}(\mathbf{q}(\mathbf{x},t))\, dx$ and numerical fluxes $\mathbf{F}\left(\mathbf{Q}_j(t), \mathbf{Q}_{j+1}(t)\right) \approx \mathbf{f}(\mathbf{q}(x_{j+1/2},t))$ yields after integration

$$\mathbf{Q}_j(t_{n+1}) = \mathbf{Q}_j(t_n) - \frac{1}{\Delta x}\int_{t_n}^{t_{n+1}} \left[\mathbf{F}\left(\mathbf{Q}_j(t), \mathbf{Q}_{j+1}(t)\right) - \mathbf{F}\left(\mathbf{Q}_{j-1}(t), \mathbf{Q}_j(t)\right)\right] dt + \int_{t_n}^{t_{n+1}} \mathbf{s}(\mathbf{Q}_j(t))\, dt$$

For instance:

$$\mathbf{Q}_j^{n+1} = \mathbf{Q}_j^n - \frac{\Delta t}{\Delta x}\left[\mathbf{F}\left(\mathbf{Q}_j^n, \mathbf{Q}_{j+1}^n\right) - \mathbf{F}\left(\mathbf{Q}_{j-1}^n, \mathbf{Q}_j^n\right)\right] + \Delta t \mathbf{s}(\mathbf{Q}_j^n)\, dt$$

Splitting methods

Solve homogeneous PDE and ODE successively!

$$\mathcal{H}^{(\Delta t)} : \quad \partial_t \mathbf{q} + \nabla \cdot \mathbf{f}(\mathbf{q}) = 0 \,, \qquad \text{IC: } \mathbf{Q}(t_m) \stackrel{\Delta t}{\Longrightarrow} \tilde{\mathbf{Q}}$$

$$\mathcal{S}^{(\Delta t)} : \quad \partial_t \mathbf{q} = \mathbf{s}(\mathbf{q}) \,, \qquad \text{IC: } \tilde{\mathbf{Q}} \stackrel{\Delta t}{\Longrightarrow} \mathbf{Q}(t_m + \Delta t)$$

1st-order Godunov splitting: $\mathbf{Q}(t_m + \Delta t) = \mathcal{S}^{(\Delta t)}\mathcal{H}^{(\Delta t)}(\mathbf{Q}(t_m))$,
2nd-order Strang splitting : $\mathbf{Q}(t_m + \Delta t) = \mathcal{S}^{(\frac{1}{2}\Delta t)}\mathcal{H}^{(\Delta t)}\mathcal{S}^{(\frac{1}{2}\Delta t)}(\mathbf{Q}(t_m))$

1st-order dimensional splitting for $\mathcal{H}^{(\cdot)}$:

$$\mathcal{X}_1^{(\Delta t)} : \quad \partial_t \mathbf{q} + \partial_{x_1} \mathbf{f}_1(\mathbf{q}) = 0 \,, \qquad \text{IC: } \mathbf{Q}(t_m) \stackrel{\Delta t}{\Longrightarrow} \tilde{\mathbf{Q}}^{1/2}$$

$$\mathcal{X}_2^{(\Delta t)} : \quad \partial_t \mathbf{q} + \partial_{x_2} \mathbf{f}_2(\mathbf{q}) = 0 \,, \qquad \text{IC: } \tilde{\mathbf{Q}}^{1/2} \stackrel{\Delta t}{\Longrightarrow} \tilde{\mathbf{Q}}$$

[Toro, 1999]

Linear upwind schemes

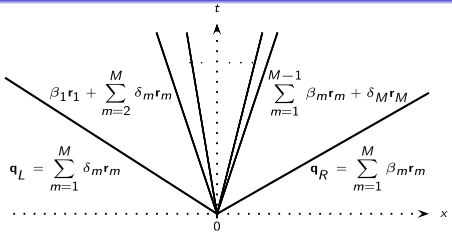

Consider Riemann problem

$$\frac{\partial}{\partial t}\mathbf{q}(x,t)+\mathbf{A}\frac{\partial}{\partial x}\mathbf{q}(x,t)=\mathbf{0}\,,\quad x\in\mathbb{R}\,,\quad t>0$$

Has exact solution

$$\mathbf{q}(x,t)=\mathbf{q}_L+\sum_{\lambda_m<x/t}a_m\mathbf{r}_m=\mathbf{q}_R-\sum_{\lambda_m\ge x/t}a_m\mathbf{r}_m=\sum_{\lambda_m\ge x/t}\delta_m\mathbf{r}_m+\sum_{\lambda_m<x/t}\beta_m\mathbf{r}_m$$

Use Riemann problem to evaluate numerical flux $\mathbf{F}(\mathbf{q}_L,\mathbf{q}_R):=\mathbf{f}(\mathbf{q}(0,t))=\mathbf{A}\mathbf{q}(0,t)$ as

$$\mathbf{F}(\mathbf{q}_L,\mathbf{q}_R)=\mathbf{A}\mathbf{q}_L+\sum_{\lambda_m<0}a_m\lambda_m\mathbf{r}_m=\mathbf{A}\mathbf{q}_R-\sum_{\lambda_m\ge 0}a_m\lambda_m\mathbf{r}_m=\sum_{\lambda_m\ge 0}\delta_m\lambda_m\mathbf{r}_m+\sum_{\lambda_m<0}\beta_m\lambda_m\mathbf{r}_m$$

Use $\quad\lambda_m^+=\max(\lambda_m,0)\,,\qquad \lambda_m^-=\min(\lambda_m,0)$

to define $\quad\mathbf{\Lambda}^+:=\mathrm{diag}(\lambda_1^+,\ldots,\lambda_M^+)\,,\qquad \mathbf{\Lambda}^-:=\mathrm{diag}(\lambda_1^-,\ldots,\lambda_M^-)$

and $\quad\mathbf{A}^+:=\mathbf{R}\,\mathbf{\Lambda}^+\,\mathbf{R}^{-1}\,,\qquad \mathbf{A}^-:=\mathbf{R}\,\mathbf{\Lambda}^-\,\mathbf{R}^{-1}\qquad$ which gives

$$\mathbf{F}(\mathbf{q}_L,\mathbf{q}_R)=\mathbf{A}\mathbf{q}_L+\mathbf{A}^-\Delta\mathbf{q}=\mathbf{A}\mathbf{q}_R-\mathbf{A}^+\Delta\mathbf{q}=\mathbf{A}^+\mathbf{q}_L+\mathbf{A}^-\mathbf{q}_R$$

with $\Delta\mathbf{q}=\mathbf{q}_R-\mathbf{q}_L$

Flux difference splitting

Godunov-type scheme with $\Delta\mathbf{Q}^n_{j+1/2} = \mathbf{Q}^n_{j+1} - \mathbf{Q}^n_j$

$$\mathbf{Q}^{n+1}_j = \mathbf{Q}^n_j - \frac{\Delta t}{\Delta x}\left(\mathbf{A}^-\Delta\mathbf{Q}^n_{j+1/2} + \mathbf{A}^+\Delta\mathbf{Q}^n_{j-1/2}\right)$$

Use linearization $\bar{\mathbf{f}}(\bar{\mathbf{q}}) = \hat{\mathbf{A}}(\mathbf{q}_L, \mathbf{q}_R)\bar{\mathbf{q}}$ and construct scheme for nonlinear problem as

$$\mathbf{Q}^{n+1}_j = \mathbf{Q}^n_j - \frac{\Delta t}{\Delta x}\left(\hat{\mathbf{A}}^-(\mathbf{Q}^n_j, \mathbf{Q}^n_{j+1})\Delta\mathbf{Q}^n_{j+\frac{1}{2}} + \hat{\mathbf{A}}^+(\mathbf{Q}^n_{j-1}, \mathbf{Q}^n_j)\Delta\mathbf{Q}^n_{j-\frac{1}{2}}\right)$$

stability condition $\max\limits_{j\in\mathbb{Z}} |\hat{\lambda}_{m,j+\frac{1}{2}}| \dfrac{\Delta t}{\Delta x} \le 1\,,\quad$ for all $m = 1, \dots, M$

Choosing $\hat{\mathbf{A}}(\mathbf{q}_L, \mathbf{q}_R)$ [Roe, 1981]:

(i) $\hat{\mathbf{A}}(\mathbf{q}_L, \mathbf{q}_R)$ has real eigenvalues (ii) $\hat{\mathbf{A}}(\mathbf{q}_L, \mathbf{q}_R) \to \dfrac{\partial\mathbf{f}(\mathbf{q})}{\partial\mathbf{q}}$ as $\mathbf{q}_L, \mathbf{q}_R \to \mathbf{q}$

(iii) $\hat{\mathbf{A}}(\mathbf{q}_L, \mathbf{q}_R)\Delta\mathbf{q} = \mathbf{f}(\mathbf{q}_R) - \mathbf{f}(\mathbf{q}_L)$

Wave decomposition: $\Delta\mathbf{q} = \mathbf{q}_r - \mathbf{q}_l = \sum\limits_m a_m\,\hat{\mathbf{r}}_m$

$$\mathbf{F}(\mathbf{q}_L, \mathbf{q}_R) = \mathbf{f}(\mathbf{q}_L) + \sum_{\hat{\lambda}_m<0} \hat{\lambda}_m\, a_m\,\hat{\mathbf{r}}_m = \mathbf{f}(\mathbf{q}_R) - \sum_{\hat{\lambda}_m\ge 0} \hat{\lambda}_m\, a_m\,\hat{\mathbf{r}}_m = \frac{1}{2}\left(\mathbf{f}(\mathbf{q}_L) + \mathbf{f}(\mathbf{q}_R) - \sum_m |\hat{\lambda}_m|\, a_m\,\hat{\mathbf{r}}_m\right)$$

Wave Propagation approach

The Wave Propagation Method [LeVeque, 1997] is built on the flux differencing approach $\mathcal{A}^{\pm}\Delta := \hat{\mathbf{A}}^{\pm}(\mathbf{q}_L, \mathbf{q}_R)\Delta\mathbf{q}$ and the *waves* $\mathcal{W}_m := a_m \hat{\mathbf{r}}_m$, i.e.

$$\mathcal{A}^-\Delta\mathbf{q} = \sum_{\hat{\lambda}_m<0} \hat{\lambda}_m \mathcal{W}_m \; , \quad \mathcal{A}^+\Delta\mathbf{q} = \sum_{\hat{\lambda}_m\geq 0} \hat{\lambda}_m \mathcal{W}_m$$

1D: $\mathbf{Q}^{n+1} = \mathbf{Q}_j^n - \dfrac{\Delta t}{\Delta x}\left(\mathcal{A}^-\Delta_{j+\frac{1}{2}} + \mathcal{A}^+\Delta_{j-\frac{1}{2}}\right) - \dfrac{\Delta t}{\Delta x}\left(\tilde{\mathbf{F}}_{j+\frac{1}{2}} - \tilde{\mathbf{F}}_{j-\frac{1}{2}}\right)$

Writing $\tilde{\mathcal{A}}^{\pm}\Delta_{j\pm 1/2} := \mathcal{A}^+\Delta_{j\pm 1/2} + \tilde{\mathbf{F}}_{j\pm 1/2}$ one can develop a truly two-dimensional one-step method [Langseth and LeVeque, 2000]

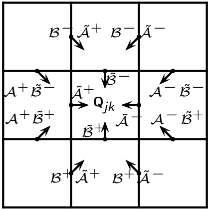

$$\begin{aligned}\mathbf{Q}_{jk}^{n+1} = \mathbf{Q}_{jk}^n &- \frac{\Delta t}{\Delta x_1}\Bigg(\tilde{\mathcal{A}}^-\Delta_{j+\frac{1}{2},k} - \frac{1}{2}\frac{\Delta t}{\Delta x_2}\left[\mathcal{A}^-\tilde{\mathcal{B}}^-\Delta_{j+1,k+\frac{1}{2}} + \mathcal{A}^-\tilde{\mathcal{B}}^+\Delta_{j+1,k-\frac{1}{2}}\right] + \\ &\qquad \tilde{\mathcal{A}}^+\Delta_{j-\frac{1}{2},k} - \frac{1}{2}\frac{\Delta t}{\Delta x_2}\left[\mathcal{A}^+\tilde{\mathcal{B}}^-\Delta_{j-1,k+\frac{1}{2}} + \mathcal{A}^+\tilde{\mathcal{B}}^+\Delta_{j-1,k-\frac{1}{2}}\right]\Bigg) \\ &- \frac{\Delta t}{\Delta x_2}\Bigg(\tilde{\mathcal{B}}^-\Delta_{j,k+\frac{1}{2}} - \frac{1}{2}\frac{\Delta t}{\Delta x_1}\left[\mathcal{B}^-\tilde{\mathcal{A}}^-\Delta_{j+\frac{1}{2},k+1} + \mathcal{B}^-\tilde{\mathcal{A}}^+\Delta_{j-\frac{1}{2},k+1}\right] + \\ &\qquad \tilde{\mathcal{B}}^+\Delta_{j,k-\frac{1}{2}} - \frac{1}{2}\frac{\Delta t}{\Delta x_1}\left[\mathcal{B}^+\tilde{\mathcal{A}}^-\Delta_{j+\frac{1}{2},k-1} + \mathcal{B}^+\tilde{\mathcal{A}}^+\Delta_{j-\frac{1}{2},k-1}\right]\Bigg)\end{aligned}$$

Outline

Block-structured adaptive mesh refinement (SAMR)

For simplicity $\partial_t \mathbf{q}(\mathbf{x},t) + \nabla \cdot \mathbf{f}(\mathbf{q}(\mathbf{x},t)) = 0$

- Refined blocks overlay coarser ones
- Refinement in space *and time* by factor r_l
- Block (aka patch) based data structures

+ Numerical scheme

$$\mathbf{Q}_{jk}^{n+1} = \mathbf{Q}_{jk}^{n} - \frac{\Delta t}{\Delta x_1}\left[\mathbf{F}^1_{j+\frac{1}{2},k} - \mathbf{F}^1_{j-\frac{1}{2},k}\right] - \frac{\Delta t}{\Delta x_2}\left[\mathbf{F}^2_{j,k+\frac{1}{2}} - \mathbf{F}^2_{j,k-\frac{1}{2}}\right]$$

only for single patch necessary

+ Efficient cache-reuse / vectorization possible

- Cluster-algorithm necessary

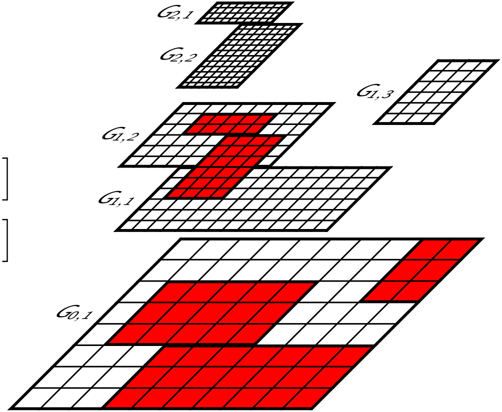

Level transfer / setting of ghost cells

Conservative averaging (restriction):

$$\hat{\mathbf{Q}}^l_{jk} := \frac{1}{(r_{l+1})^2} \sum_{\kappa=0}^{r_{l+1}-1} \sum_{\iota=0}^{r_{l+1}-1} \mathbf{Q}^{l+1}_{v+\kappa,w+\iota}$$

Bilinear interpolation (prolongation):

$$\check{\mathbf{Q}}^{l+1}_{vw} := (1-f_1)(1-f_2)\,\mathbf{Q}^l_{j-1,k-1} + f_1(1-f_2)\,\mathbf{Q}^l_{j,k-1} + (1-f_1)f_2\,\mathbf{Q}^l_{j-1,k} + f_1 f_2\,\mathbf{Q}^l_{jk}$$

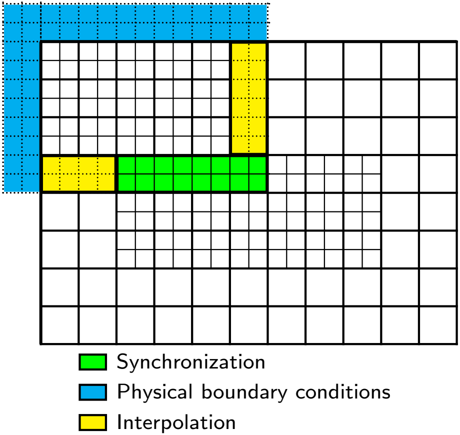

For boundary conditions: linear time interpolation

$$\tilde{\mathbf{Q}}^{l+1}(t+\kappa\Delta t_{l+1}) := \left(1-\frac{\kappa}{r_{l+1}}\right)\check{\mathbf{Q}}^{l+1}(t) + \frac{\kappa}{r_{l+1}}\check{\mathbf{Q}}^{l+1}(t+\Delta t_l) \quad \text{for } \kappa = 0,\ldots r_{l+1}$$

Conservative flux correction

Example: Cell $j,\ k$

$$\check{\mathbf{Q}}^l_{jk}(t+\Delta t_l) = \mathbf{Q}^l_{jk}(t) - \frac{\Delta t_l}{\Delta x_{1,l}}\left(\mathbf{F}^{1,l}_{j+\frac{1}{2},k} - \frac{1}{r^2_{l+1}}\sum_{\kappa=0}^{r_{l+1}-1}\sum_{\iota=0}^{r_{l+1}-1}\mathbf{F}^{1,l+1}_{v+\frac{1}{2},w+\iota}(t+\kappa\Delta t_{l+1})\right) - \frac{\Delta t_l}{\Delta x_{2,l}}\left(\mathbf{F}^{2,l}_{j,k+\frac{1}{2}} - \mathbf{F}^{2,l}_{j,k-\frac{1}{2}}\right)$$

Correction pass:

1. $\delta\mathbf{F}^{1,l+1}_{j-\frac{1}{2},k} := -\mathbf{F}^{1,l}_{j-\frac{1}{2},k}$
2. $\delta\mathbf{F}^{1,l+1}_{j-\frac{1}{2},k} := \delta\mathbf{F}^{1,l+1}_{j-\frac{1}{2},k} + \frac{1}{r^2_{l+1}}\sum_{\iota=0}^{r_{l+1}-1}\mathbf{F}^{1,l+1}_{v+\frac{1}{2},w+\iota}(t+\kappa\Delta t_{l+1})$
3. $\check{\mathbf{Q}}^l_{jk}(t+\Delta t_l) := \mathbf{Q}^l_{jk}(t+\Delta t_l) + \frac{\Delta t_l}{\Delta x_{1,l}}\,\delta\mathbf{F}^{1,l+1}_{j-\frac{1}{2},k}$

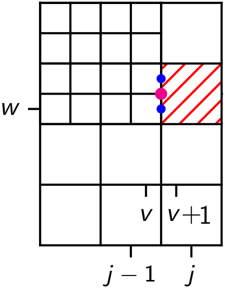

The basic recursive algorithm

```
AdvanceLevel(l)

  Repeat r_l times
      Set ghost cells of Q^l(t)
      If time to regrid?
          Regrid(l)
      UpdateLevel(l)
      If level l+1 exists?
          Set ghost cells of Q^l(t+Δt_l)
          AdvanceLevel(l+1)
          Average Q^(l+1)(t+Δt_l) onto Q^l(t+Δt_l)
          Correct Q^l(t+Δt_l) with δF^(l+1)
      t := t+Δt_l
```

[Berger and Colella, 1988][Berger and Oliger, 1984]

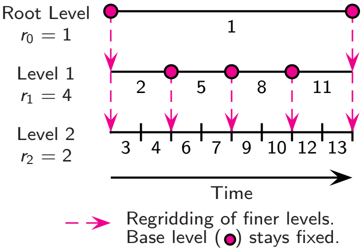

Heuristic error estimation for FV methods

$$\tau \approx \frac{|\mathcal{R}\mathcal{H}_2^{\Delta t_l}\,\mathbf{Q}^l(t_l-\Delta t_l) - \mathcal{H}^{2\Delta t_l}\,\mathcal{R}\mathbf{Q}^l(t_l-\Delta t_l)|}{2^{o+1}-2}$$

2. Create temporary Grid coarsened by factor 2
   Initialize with fine-grid-values of preceding time step

1. Error estimation on interior cells

3. Compare temporary solutions

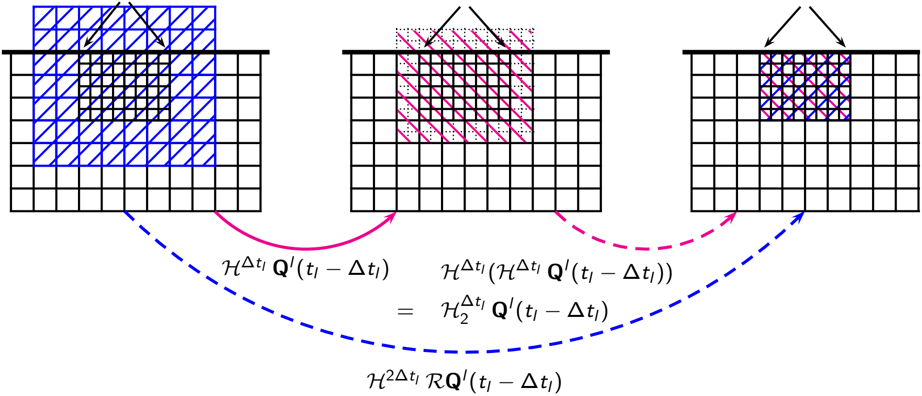

Level-set method for boundary embedding

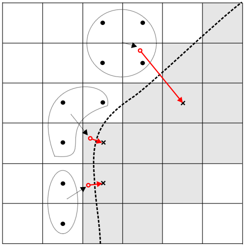

- Implicit boundary representation via distance function φ, normal $\mathbf{n} = \nabla\varphi / |\nabla\varphi|$
- Complex boundary moving with local velocity $\mathbf{w}$, treat interface as moving rigid wall
- Construction of values in embedded boundary cells by interpolation / extrapolation

Interpolate / constant value extrapolate values at

$$\tilde{\mathbf{x}} = \mathbf{x} + 2\varphi\mathbf{n}$$

Velocity in ghost cells

$$\mathbf{u}' = (2\mathbf{w}\cdot\mathbf{n} - \mathbf{u}\cdot\mathbf{n})\mathbf{n} + (\mathbf{u}\cdot\mathbf{t})\mathbf{t}$$
$$= 2\left((\mathbf{w} - \mathbf{u})\cdot\mathbf{n}\right)\mathbf{n} + \mathbf{u}$$

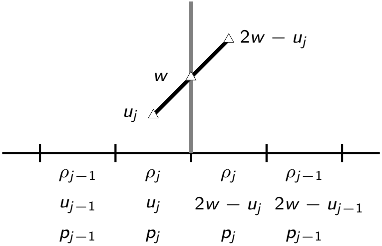

Accuracy test: stationary vortex

Construct non-trivial *radially symmetric* and *stationary* solution by balancing hydrodynamic pressure and centripetal force per volume element, i.e.

$$\frac{d}{dr}p(r) = \rho(r)\frac{U(r)^2}{r}$$

For $\rho_0 \equiv 1$ and the velocity field

$$U(r) = \alpha \cdot \begin{cases} 2r/R & \text{if } 0 < r < R/2, \\ 2(1 - r/R) & \text{if } R/2 \le r \le R, \\ 0 & \text{if } r > R, \end{cases}$$

Compute one full rotation, Roe solver, embedded slip wall boundary conditions

$x_{1,c} = 0.5,\ x_{2,c} = 0.5,\ R = 0.4,\ t_{end} = 1,\ \Delta h = \Delta x_1 = \Delta x_2 = 1/N,\ \alpha = R\pi$

$U(r)$

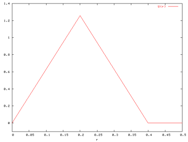

$p(r)$

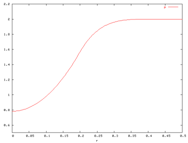

Marginal shear flow along boundary, $R_G = R$

N	Wave Propagation		Godunov Splitting	
	Error	Order	Error	Order
20	0.0120056		0.0144203	
40	0.0035074	1.78	0.0073070	0.98
80	0.0014193	1.31	0.0038401	0.93
160	0.0005032	1.50	0.0018988	1.02

Major shear flow along boundary, $R_G = R/2$

N	Wave Propagation		Godunov Splitting	
	Error	Order	Error	Order
20	0.0423925		0.0271446	
40	0.0358735	0.24	0.0242260	0.16
80	0.0212340	0.76	0.0128638	0.91
160	0.0121089	0.81	0.0070906	0.86

Verification: shock reflection

- Reflection of a Mach 2.38 shock in nitrogen at 43^o wedge
- 2nd order MUSCL scheme with Roe solver, 2nd order multidimensional wave propagation method

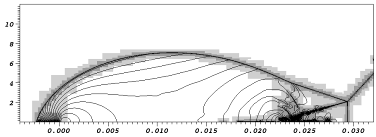

Cartesian base grid 360 $\times$ 160 cells on domain of $36\,\mathrm{mm} \times 16\,\mathrm{mm}$ with up to 3 refinement levels with $r_l = 2, 4, 4$ and $\Delta x_{1,2} = 3.125\mu m$, $38\,\mathrm{h}$ CPU

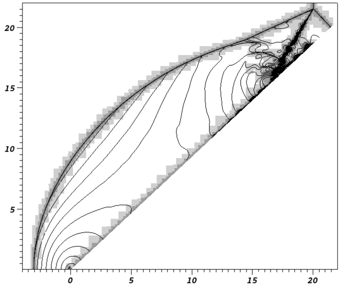

GFM base grid 390 $\times$ 330 cells on domain of $26\,\mathrm{mm} \times 22\,\mathrm{mm}$ with up to 3 refinement levels with $r_l = 2, 4, 4$ and $\Delta x_{e,1,2} = 2.849\mu m$, $200\,\mathrm{h}$ CPU

Shock reflection: SAMR solution for Euler equations

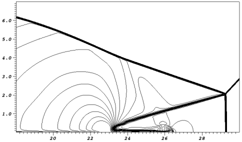

$\Delta x = 25\,\mathrm{mm}$

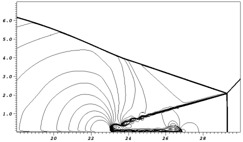

$\Delta x = 12.5\,\mathrm{mm}$

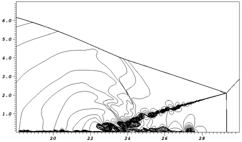

$\Delta x = 3.125\,\mathrm{mm}$

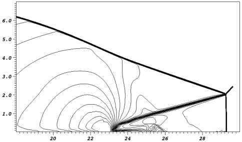

$\Delta x_e = 22.8\,\mathrm{mm}$

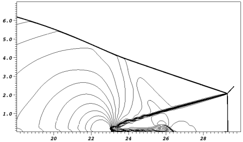

$\Delta x_e = 11.4\,\mathrm{mm}$

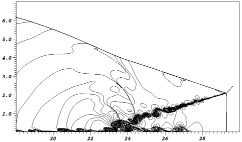

$\Delta x_e = 2.849\,\mathrm{mm}$

2nd order MUSCL scheme with Van Leer FVS, dimensional splitting

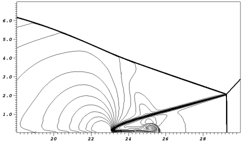

$\Delta x = 12.5\,\mathrm{mm}$

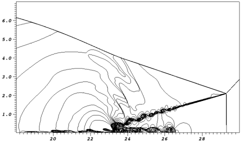

$\Delta x = 3.125\,\mathrm{mm}$

Parallelization strategies

Decomposition of the hierarchical data
Separate distribution of each level, cf. [Rendleman et al., 2000]
Rigorous domain decomposition

- Data of all levels resides on same node
- Grid hierarchy defines unique "floor-plan"
- Workload estimation

$$\mathcal{W}(\Omega) = \sum_{l=0}^{l_{\max}} \left[\mathcal{N}_l(G_l \cap \Omega) \prod_{\kappa=0}^{l} r_\kappa \right]$$

- Parallel operations
  - Synchronization of ghost cells
  - Redistribution of data blocks within regridding operation
  - Flux correction of coarse grid cells

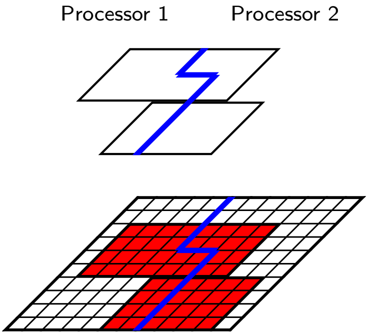

RD (2005). *Adaptive Mesh Refinement - Theory and Applications*, pages 361–372. Springer

Space-filling curve algorithm

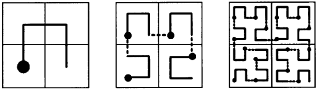

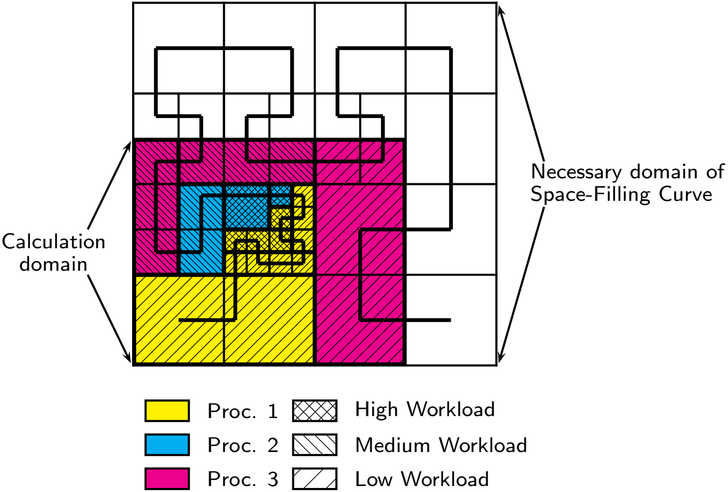

Partitioning example

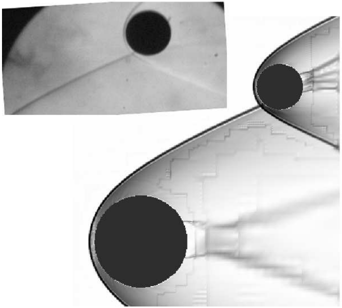

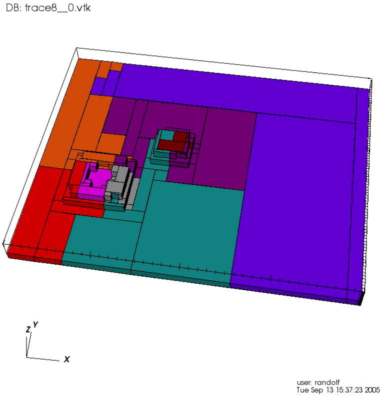

- Cylinders of spheres in supersonic flow
- Predict force on secondary body
- Right: 200x160 base mesh, 3 Levels, factors 2,2,2, 8 CPUs

S. J. Laurence, RD, and H. G. Hornung, H. G. (2007). *J. Fluid Mech.*, 590:209–237

Outline

Governing equations for premixed combustion

Euler equations with reaction terms

$$\frac{\partial \rho_i}{\partial t} + \frac{\partial}{\partial x_n}(\rho_i u_n) = \dot{\omega}_i \;, \quad i = 1, \dots, K$$
$$\frac{\partial}{\partial t}(\rho u_k) + \frac{\partial}{\partial x_n}(\rho u_k u_n + \delta_{kn} p) = 0 \;, \quad k = 1, \dots, d$$
$$\frac{\partial}{\partial t}(\rho E) + \frac{\partial}{\partial x_n}(u_n(\rho E + p)) = 0$$

Ideal gas law and Dalton's law for gas-mixtures

$$p(\rho_1, \dots, \rho_K, T) = \sum_{i=1}^{K} p_i = \sum_{i=1}^{K} \rho_i \frac{\mathcal{R}}{W_i} T = \rho \frac{\mathcal{R}}{W} T \quad \text{with} \quad \sum_{i=1}^{K} \rho_i = \rho \,, \, Y_i = \frac{\rho_i}{\rho}$$

Caloric equation $h(Y_1, \dots, Y_K, T) = \sum_{i=1}^{K} Y_i h_i(T)$ with $h_i(T) = h_i^0 + \int_0^T c_{pi}(s) ds$

Iterative computation of $T = T(\rho_1, \dots, \rho_K, e)$ from implicit equation

$$\sum_{i=1}^{K} \rho_i \, h_i(T) - \mathcal{R} T \sum_{i=1}^{K} \frac{\rho_i}{W_i} - \rho e = 0$$

Arrhenius-Kinetics

$$\dot{\omega}_i = \sum_{j=1}^{M} (\nu_{ji}^r - \nu_{ji}^f) \left[k_j^f \prod_{n=1}^{K} \left(\frac{\rho_n}{W_n} \right)^{\nu_{jn}^f} - k_j^r \prod_{n=1}^{K} \left(\frac{\rho_n}{W_n} \right)^{\nu_{jn}^r} \right] \quad i = 1, \dots, K$$

Non-equilibrium mechanism for hydrogen-oxgen combustion

				A [cm, mol, s]	β	E_{act} [cal mol^{-1}]
1.	$H + O_2$	$\longrightarrow$	$O + OH$	1.86×10^{14}	0.00	16790.
2.	$O + OH$	$\longrightarrow$	$H + O_2$	1.48×10^{13}	0.00	680.
3.	$H_2 + O$	$\longrightarrow$	$H + OH$	1.82×10^{10}	1.00	8900.
4.	$H + OH$	$\longrightarrow$	$H_2 + O$	8.32×10^{09}	1.00	6950.
5.	$H_2O + O$	$\longrightarrow$	$OH + OH$	3.39×10^{13}	0.00	18350.
...	...		...	...	...	...
32.	$O + O + M$	$\longrightarrow$	$O_2 + M$	4.68×10^{15}	−0.28	0.
33.	$H_2 + M$	$\longrightarrow$	$H + H + M$	2.19×10^{14}	0.00	96000.
34.	$H + H + M$	$\longrightarrow$	$H_2 + M$	3.02×10^{15}	0.00	0.

[Westbrook, 1982]

Integration of reaction rates: ODE integration in $\mathcal{S}^{(\cdot)}$ for Euler equations with chemical reaction

- Standard implicit or semi-implicit ODE-solver subcycles within each cell
- ρ, e, u_k remain unchanged!

$$\partial_t \rho_i = W_i \dot{\omega}_i(\rho_1, \ldots, \rho_K, T) \qquad i = 1, \ldots, K$$

- Parsing of mechanism with Chemkin-II
- Evalutation of $\dot{\omega}_i$ with automatically generated optimized Fortran-77 functions in the line of Chemkin-II

RD and G. Bader (2005). *Analysis and Numerics for Conservation Laws*, pages 69–91, Springer

Riemann solver for combustion

(S1) Calculate standard Roe-averages $\hat{\rho}$, $\hat{u}_n$, $\hat{H}$, $\hat{Y}_i$, $\hat{T}$.

(S2) Compute $\hat{\gamma} := \hat{c}_p/\hat{c}_v$ with $\hat{c}_{\{p/v\}i} = \dfrac{1}{T_R - T_L} \displaystyle\int_{T_L}^{T_R} c_{\{p,v\}i}(\tau)\, d\tau$.

(S3) Calculate $\hat{\phi}_i := (\hat{\gamma} - 1)\left(\frac{\hat{\mathbf{u}}^2}{2} - \hat{h}_i\right) + \hat{\gamma}\, R_i\, \hat{T}$ with standard Roe-averages $\hat{e}_i$ or $\hat{h}_i$.

(S4) Calculate $\hat{c} := \left(\sum_{i=1}^{K} \hat{Y}_i\, \hat{\phi}_i - (\hat{\gamma} - 1)\hat{\mathbf{u}}^2 + (\hat{\gamma} - 1)\hat{H}\right)^{1/2}$.

(S5) Use $\Delta\mathbf{q} = \mathbf{q}_R - \mathbf{q}_L$ and Δp to compute the wave strengths a_m.

(S6) Calculate $\mathcal{W}_1 = a_1 \hat{\mathbf{r}}_1$, $\mathcal{W}_2 = \displaystyle\sum_{\iota=2}^{K+d} a_\iota \hat{\mathbf{r}}_\iota$, $\mathcal{W}_3 = a_{K+d+1} \hat{\mathbf{r}}_{K+d+1}$.

(S7) Evaluate $s_1 = \hat{u}_1 - \hat{c}$, $s_2 = \hat{u}_1$, $s_3 = \hat{u}_1 + \hat{c}$.

(S8) Evaluate $\rho^\star_{L/R}$, $u^\star_{1,L/R}$, $e^\star_{L/R}$, $c^\star_{1,L/R}$ from $\mathbf{q}^\star_L = \mathbf{q}_L + \mathcal{W}_1$ and $\mathbf{q}^\star_R = \mathbf{q}_R - \mathcal{W}_3$.

(S9) If $\rho^\star_{L/R} \le 0$ or $e^\star_{L/R} \le 0$ use $\mathbf{F}_{HLL}(\mathbf{q}_L, \mathbf{q}_R)$ and go to (S12).

(S10) Entropy correction: Evaluate $|\tilde{s}_\iota|$.
$\mathbf{F}_{Roe}(\mathbf{q}_L, \mathbf{q}_R) = \frac{1}{2}\left(\mathbf{f}(\mathbf{q}_L) + \mathbf{f}(\mathbf{q}_R) - \sum_{\iota=1}^{3} |\tilde{s}_\iota| \mathcal{W}_\iota\right)$

(S11) Positivity correction: Replace $\mathbf{F}_i$ by

$$\mathbf{F}_i^\star = \mathbf{F}_\rho \cdot \begin{cases} Y_i^l\,, & \mathbf{F}_\rho \ge 0\,, \\ Y_i^r\,, & \mathbf{F}_\rho < 0\,. \end{cases}$$

(S12) Evaluate maximal signal speed by $S = \max(|s_1|, |s_3|)$.

RD (2006). Proc. Tenth Int. Conf. Hyperbolic Problems, pages 343–350, Yokohama Publishers

Riemann solver for combustion: carbuncle fix

Entropy correction [Harten, 1983]

$$|\tilde{s}_\iota| = \begin{cases} |s_\iota| & \text{if} |s_\iota| \geq 2\eta \\ \frac{|s_\iota^2|}{4\eta} + \eta & \text{otherwise} \end{cases}$$

$$\eta = \frac{1}{2} \max_\iota \left\{ |s_\iota(\mathbf{q}_R) - s_\iota(\mathbf{q}_L)| \right\}$$

2D modification of entropy correction [Sanders et al., 1998]:

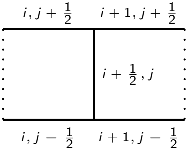

$$\tilde{\eta}_{i+1/2,j} = \max \left\{ \eta_{i+1/2,j}, \eta_{i,j-1/2}, \ \eta_{i,j+1/2}, \eta_{i+1,j-1/2}, \eta_{i+1,j+1/2} \right\}$$

Carbuncle phenomenon

- [Quirk, 1994]

RD (2003). *Parallel adaptive simulation of multi-dimensional detonation structures*, PhD thesis

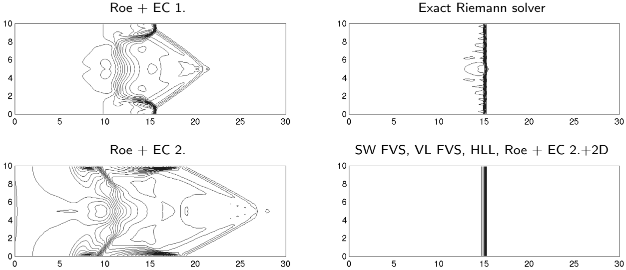

Detonation ignition in a shock tube

- Shock-induced detonation ignition of $\mathrm{H_2} : \mathrm{O_2} : \mathrm{Ar}$ mixture at molar ratios 2:1:7 in closed 1d shock tube
- Insufficient resolution leads to inaccurate results
- Reflected shock is captured correctly by FV scheme, detonation is resolution dependent
- Fine mesh necessary in the induction zone at the head of the detonation

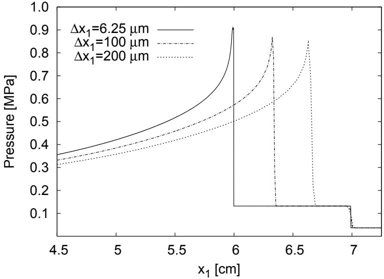

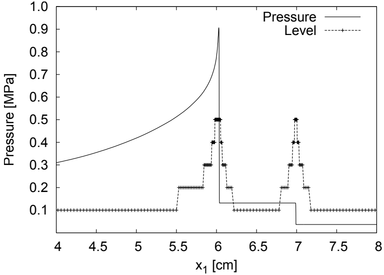

Pressure distribution $t = 170\,\mu\mathrm{s}$ after ignition.Right: Domains of refinement levels

Shock-induced combustion around a sphere

- Spherical projectile of radius $1.5\,\mathrm{mm}$ travels with constant velocity $v_I = 2170.6\,\mathrm{m/s}$ through $\mathrm{H_2}:\mathrm{O_2}:\mathrm{Ar}$ mixture (molar ratios 2:1:7) at $6.67\,\mathrm{kPa}$ and $T = 298\,\mathrm{K}$
- Cylindrical symmetric simulation on AMR base mesh of 70×40 cells

3-level computation with $r_{1,2} = 2$

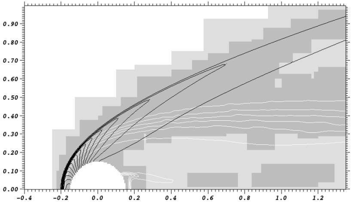

4-level computation with $r_{1,2} = 2$, $r_3 = 4$

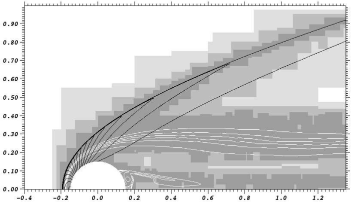

4-level distribution

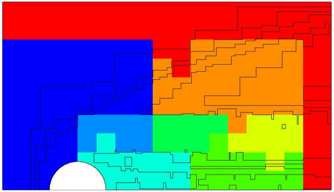

4-level refinement flags

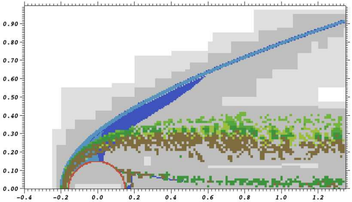

RD (2009). *Computers & Structures* 87:769–783.

Detonation diffraction

- Simulation of CJ detonation for $H_2 : O_2 : Ar / 2 : 1 : 7$ at $T_0 = 298\,\mathrm{K}$ and $p_0 = 10\,\mathrm{kPa}$, experiment by J. Shepherd et al. for $H_2 : O_2 : N_2$
- $25\,\mathrm{Pts}/l_{ig}$. Base grid 508×288, 4 additional refinement levels (2,2,2,4), $\sim 3850\,\mathrm{h}$ CPU on 48 nodes Athlon 1.4GHz
- Adaptive computations use up to $\sim 2.2\,\mathrm{M}$ instead of $\sim 150\,\mathrm{M}$ cells (uniform grid)

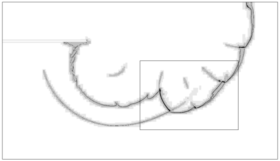

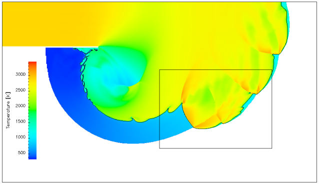

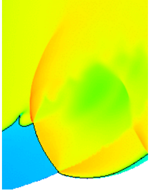

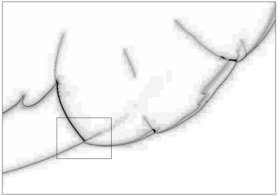

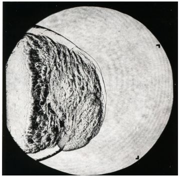

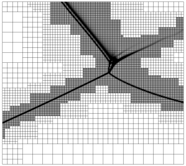

Outline

Construction of coupling data

- Moving boundary/interface is treated as a moving contact discontinuity and represented by level set [Fedkiw, 2002][Arienti et al., 2003]
- One-sided construction of mirrored ghost cell and new FEM nodal point values
- FEM ansatz-function interpolation to obtain intermediate surface values
- Explicit coupling possible if geometry and velocities are prescribed for the more compressible medium [Specht, 2000]

$u_n^F := u_n^S(t)|_{\mathcal{I}}$
UpdateFluid(Δt)
$\sigma_{nn}^S := p^F(t+\Delta t)|_{\mathcal{I}}$
UpdateSolid(Δt)
$t := t + \Delta t$

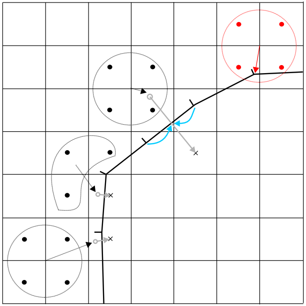

Coupling conditions on interface

$$\left.\begin{array}{rcl} u_n^S & = & u_n^F \\ \sigma_{nn}^S & = & p^F \\ \sigma_{nm}^S & = & 0 \end{array}\right|_{\mathcal{I}}$$

Usage of SAMR

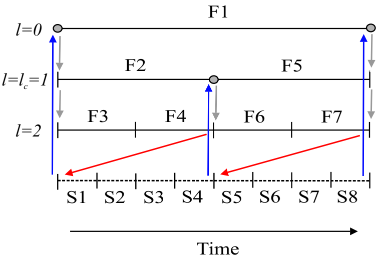

- Eulerian SAMR + non-adaptive Lagrangian FEM scheme
- Exploit SAMR time step refinement for effective coupling to solid solver
  - Lagrangian simulation is called only at level $l_c \leq l_{\max}$
  - SAMR refines solid boundary at least at level l_c
  - Additional levels can be used resolve geometric ambiguities
- Nevertheless: Inserting sub-steps accommodates for time step reduction from the solid solver within an SAMR cycle
- Communication strategy:
  - Updated boundary info from solid solver must be received before regridding operation
  - Boundary data is sent to solid when highest level available
- Inter-solver communication (point-to-point or globally) managed on the fly by special coupling module

RD, R. Radovitzky, S. P. Mauch et al. (2006). *Engineering with Computers* 22(3-4):325–347

Rigid body motion: lift-up of a spherical body

Cylindrical body hit by Mach 3 shockwave, 2D test case by [Falcovitz et al., 1997]

Schlieren plot of density

Refinement levels

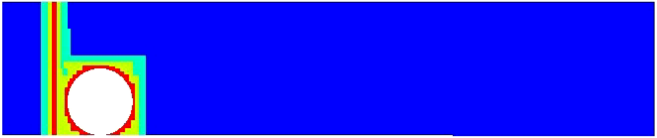

Closest point transform algorithm

The signed distance φ to a surface $\mathcal{I}$ satisfies the eikonal equation [Sethian, 1999]

$$|\nabla\varphi| = 1 \quad \text{with} \quad \varphi\big|_{\mathcal{I}} = 0$$

Solution smooth but non-diferentiable across characteristics.

Distance computation trivial for non-overlapping elementary shapes but difficult to do efficiently for triangulated surface meshes:

- Geometric solution approach with plosest-point-transform algorithm [Mauch, 2003]

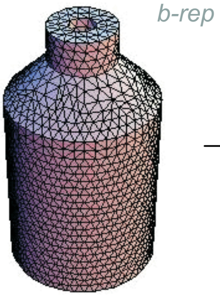

Surface mesh $\mathcal{I}$

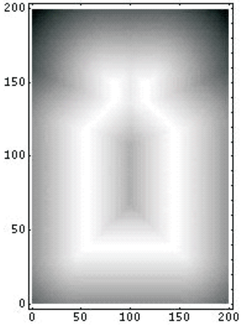

Distance φ

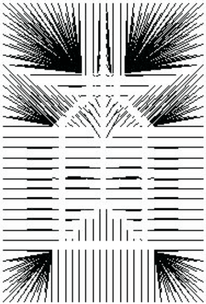

Normal to closest point

Eulerian/Lagrangian communication module

1. Put bounding boxes around each solid processors piece of the boundary and around each fluid processors grid
2. Gather, exchange and broadcast of bounding box information
3. Optimal point-to-point communication pattern, non-blocking

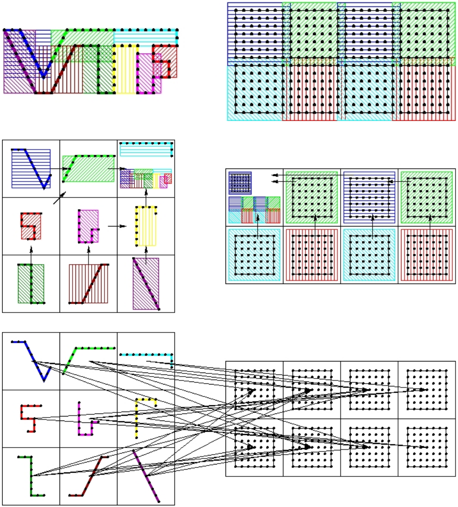

RD, R. Radovitzky, S. P. Mauch et al. (2006). *Engineering with Computers* 22(3-4):325–347

Treatment of thin structures

- Thin boundary structures or lower-dimensional shells require "thickening" to apply embedded boundary method
- Unsigned distance level set function φ
- Treat cells with $0 < \varphi < d$ as ghost fluid cells

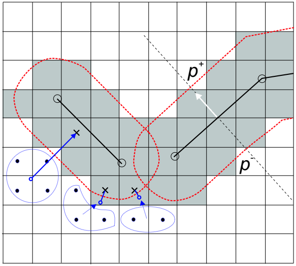

- Leaving φ unmodified ensures correctness of $\nabla\varphi$
- Use face normal in shell element to evaluate in $\Delta p = p^+ - p^-$

Test case suggested by [Giordano et al., 2005]

- Forward facing step geometry, fixed walls everywhere except at inflow

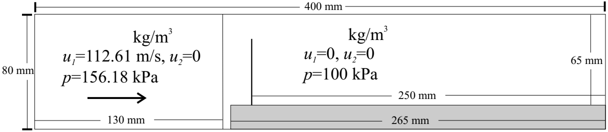

Shock-driven elastic panel motion

- Thin steel plate (thickness $h = 1\,\mathrm{mm}$, length $50\,\mathrm{mm}$), clamped at lower end
- $\rho_s = 7600\,\mathrm{kg/m^3}$, $E = 220\,\mathrm{GPa}$, $I = h^3/12$, $\nu = 0.3$
- SAMR base mesh $320 \times 64(\times 2)$, $r_{1,2} = 2$, $l_c = 2$, 4 solid sub-iterations
- Intel 3.4GHz Xeon dual processors, GB Ethernet interconnect
  - $\sim 450\,\mathrm{h}$ CPU on 15 fluid CPU + 1 solid CPU for DYNA3D

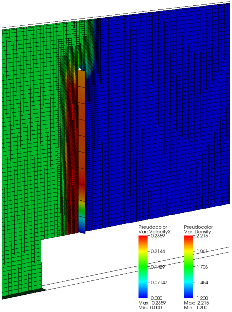

$t \approx 0.06\,\mathrm{ms}$

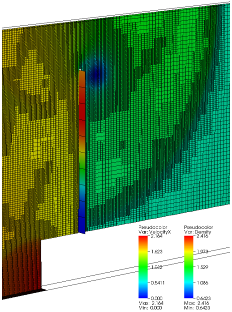

$t \approx 0.24\,\mathrm{ms}$

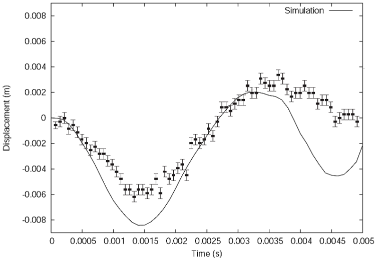

Tip displacement in simulation and experiment

RD. CNMAC '10 Proceedings

Two-phase model

Volume fraction based two-component model with $\sum_{i=1}^{m} \alpha^i = 1$, that defines mixture quantities as

$$\rho = \sum_{i=1}^{m} \alpha^i \rho^i \; , \quad \rho u_n = \sum_{i=1}^{m} \alpha^i \rho^i u_n^i \; , \quad \rho e = \sum_{i=1}^{m} \alpha^i \rho^i e^i$$

Assuming total pressure $p = (\gamma - 1)\,\rho e - \gamma p_\infty$ and speed of sound $c = (\gamma\,(p + p_\infty)/\rho)^{1/2}$ yields

$$\frac{p}{\gamma - 1} = \sum_{i=1}^{m} \frac{\alpha^i p^i}{\gamma^i - 1} \; , \quad \frac{\gamma p_\infty}{\gamma - 1} = \sum_{i=1}^{m} \frac{\alpha^i \gamma^i p_\infty^i}{\gamma^i - 1}$$

and the overall set of equations [Shyue, 1998]

$$\partial_t \rho + \partial_{x_n}(\rho u_n) = 0 \; , \quad \partial_t(\rho u_k) + \partial_{x_n}(\rho u_k u_n + \delta_{kn} p) = 0 \; , \quad \partial_t(\rho E) + \partial_{x_n}(u_n(\rho E + p)) = 0$$

$$\frac{\partial}{\partial t}\left(\frac{1}{\gamma - 1}\right) + u_n \frac{\partial}{\partial x_n}\left(\frac{1}{\gamma - 1}\right) = 0 \; , \quad \frac{\partial}{\partial t}\left(\frac{\gamma p_\infty}{\gamma - 1}\right) + u_n \frac{\partial}{\partial x_n}\left(\frac{\gamma p_\infty}{\gamma - 1}\right) = 0$$

Oscillation free at contacts: [Abgrall and Karni, 2001][Shyue, 2006]

Approximate Riemann solver

Use HLLC approach because of robustness and positivity preservation

$$\mathbf{q}^{HLLC}(x_1,t) = \begin{cases} \mathbf{q}_L\,, & x_1 < s_L\, t, \\ \mathbf{q}_L^\star\,, & s_L\, t \le x_1 < s^\star\, t, \\ \mathbf{q}_R^\star\,, & s^\star\, t \le x_1 \le s_R\, t, \\ \mathbf{q}_R\,, & x_1 > s_R\, t, \end{cases}$$

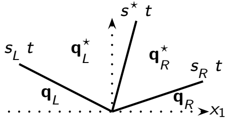

Wave speed estimates [Davis, 1988] $s_L = \min\{u_{1,L} - c_L, u_{1,R} - c_R\}$,
$s_R = \max\{u_{1,L} + c_L, u_{1,R} + c_R\}$
Unkown state [Toro et al., 1994]

$$s^\star = \frac{p_R - p_L + s_L u_{1,L}(s_L - u_{1,L}) - \rho_R u_{1,R}(s_R - u_{1,R})}{\rho_L(s_L - u_{1,L}) - \rho_R(s_R - u_{1,R})}$$

$$\mathbf{q}_\tau^\star = \left[\eta, \eta s^\star, \eta u_2, \eta\left[\frac{(\rho E)_\tau}{\rho_\tau} + (s^\star - u_{1,\tau})\left(s_\tau + \frac{p_\tau}{\rho_\tau(s_\tau - u_{1,\tau})}\right)\right], \frac{1}{\gamma_\tau - 1}, \frac{\gamma_\tau p_{\infty,\tau}}{\gamma_\tau - 1}\right]^T$$

$$\eta = \rho_\tau \frac{s_\tau - u_{1,\tau}}{s_\tau - s^\star}\,, \quad \tau = \{L, R\}$$

Evaluate waves as $\mathcal{W}_1 = \mathbf{q}_L^\star - \mathbf{q}_L$, $\mathcal{W}_2 = \mathbf{q}_R^\star - \mathbf{q}_L^\star$, $\mathcal{W}_3 = \mathbf{q}_R - \mathbf{q}_R^\star$ and $\lambda_1 = s_L$, $\lambda_2 = s^\star$, $\lambda_3 = s_R$ to compute the fluctuations $\mathcal{A}^-\Delta = \sum_{\lambda_\nu < 0} \lambda_\nu\, \mathcal{W}_\nu$, $\mathcal{A}^+\Delta = \sum_{\lambda_\nu \ge 0} \lambda_\nu\, \mathcal{W}_\nu$ for $\nu = \{1, 2, 3\}$

Overall scheme: Wave Propagation method [Shyue, 2006]

Plate in water shocktube

- Air: $\gamma^A = 1.4$, $p_\infty^A = 0$, $\rho^A = 1.29\,\mathrm{kg/m^3}$
- Water: $\gamma^W = 7.415$, $p_\infty^W = 296.2\,\mathrm{MPa}$, $\rho^W = 1027\,\mathrm{kg/m^3}$
- Cavitation modeling with pressure cut-off model at $p = -1\,\mathrm{MPa}$
- 3D simulation of copper plate $r = 32\,\mathrm{mm}$, $h = 0.25\,\mathrm{mm}$ deforming and rupturing rupturing due to water hammer
  - Water-filled shocktube $1.3\,\mathrm{m}$ with driver piston [Deshpande et al., 2006]
  - Piston simulated with separate level set
  - $\rho_s = 8920\,\mathrm{kg/m3}$, $E = 130\,\mathrm{GPa}$, $\nu = 0.31$, yield stress $\sigma_y = 38.5\,\mathrm{MPa}$
  - $350 \times 20 \times 20$, $r_{1,2} = 2$, $l_c = 2$
- DYNA3D: 327 triangles, tangent modulus $E_T = 3\,\mathrm{GPa}$, hardening parameter $\beta = 0.5$ for material model $\#3$
- SFC: 8896 triangles, J2 plasticity model

Plastic plastic deformation

- $p_0 = 34\,\mathrm{MPa}$
- AMROC-DYNA3D: 15+1 processors 3.4 GHz Intel Xeon dual, 2192 coupled steps, $\sim 97\,\mathrm{h}$ CPU, RD. CNMAC '10 Proceedings.
- AMROC-SFC: 12+4 processors 3.4 GHz Intel Xeon dual, 2000 coupled steps, $\sim 130\,\mathrm{h}$ CPU

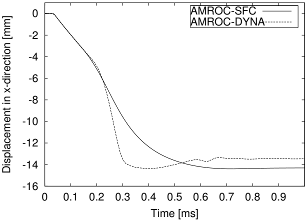

Plate center displacement

AMROC-DYNA3D: Solid velocity v_1 and fluid pressure p

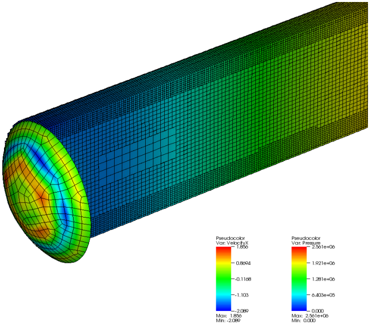

RD. CNMAC '10 Proceedings

AMROC-SFC: Deformed plate at end of simulation at $t_e = 1.0\,\mathrm{ms}$

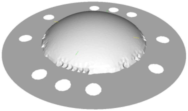

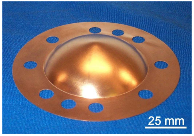

RD, F. Cirak, S. P. Mauch, and D. I. Meiron (2007). *Int. J. Multiscale Computational Engineering*, 5(1):47–63

Plate fracture

- AMR base mesh $374 \times 20 \times 20$, $r_{1,2} = 2$, $l_c = 2$
- ~ 1250 coupled time steps to $t_{end} = 1\,\mathrm{ms}$
- 12+12 processors 3.4 GHz Intel Xeon, $\sim 800\,\mathrm{h}$ CPU, cohesive interface model, max. tensile stress $\sigma_c = 525\,\mathrm{MPa}$

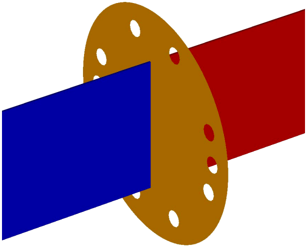

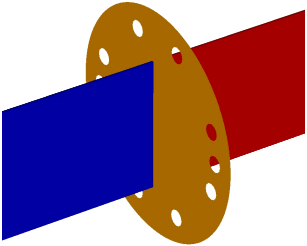

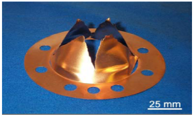

$p_0 = 64\,\mathrm{MPa}$

$p_0 = 173\,\mathrm{MPa}$

RD, F. Cirak, and S. P. Mauch (2009). *Int. Workshop on Fluid-Structure Interaction. Theory, Numerics and Applications, Herrsching am Ammersee 2008*, pages 65–80. kassel university press GmbH.

Detonation-driven plastic deformation

Chapman-Jouguet detonation in a tube filled with a stoichiometric ethylene and oxygen ($\mathrm{C_2H_4} + 3\,\mathrm{O_2}$, 295 K) mixture. Euler equations with single exothermic reaction $A \longrightarrow B$

$$\partial_t \rho + \partial_{x_n}(\rho u_n) = 0\,, \quad \partial_t(\rho u_k) + \partial_{x_n}(\rho u_k u_n + \delta_{kn} p) = 0\,, k = 1, \dots, d$$

$$\partial_t(\rho E) + \partial_{x_n}(u_n(\rho E + p)) = 0\,, \quad \partial_t(Y\rho) + \partial_{x_n}(Y \rho u_n) = \psi$$

with

$$p = (\gamma - 1)(\rho E - \frac{1}{2}\rho u_n u_n - \rho Y q_0) \quad \text{and} \quad \psi = -kY\rho \exp\left(\frac{-E_\mathrm{A}\rho}{p}\right)$$

modeled with heuristic detonation model by [Mader, 1979]

$V := \rho^{-1},\ V_0 := \rho_0^{-1},\ V_\mathrm{CJ} := \rho_\mathrm{CJ}$
$Y' := 1 - (V - V_0)/(V_\mathrm{CJ} - V_0)$
If $0 \le Y' \le 1$ and $Y > 10^{-8}$ then
  If $Y < Y'$ and $Y' < 0.9$ then $Y' := 0$
  If $Y' < 0.99$ then $p' := (1 - Y')p_\mathrm{CJ}$
    else $p' := p$
  $\rho_\mathrm{A} := Y'\rho$
  $E := p'/(\rho(\gamma - 1)) + Y' q_0 + \frac{1}{2} u_n u_n$

Comparison of the pressure traces in the experiment and in a 1d simulation

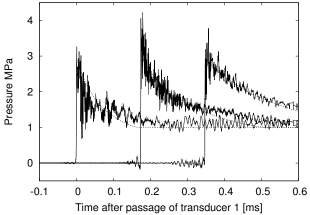

Tube with flaps

- Fluid: VanLeer flux vector splitting
  - Detonation model with $\gamma = 1.24$, $p_{\mathrm{CJ}} = 3.3\,\mathrm{MPa}$, $D_{\mathrm{CJ}} = 2376\,\mathrm{m/s}$
  - AMR base level: $104 \times 80 \times 242$, $r_{1,2} = 2$, $r_3 = 4$
  - $\sim 4 \cdot 10^7$ cells instead of $7.9 \cdot 10^9$ cells (uniform)
  - Tube and detonation fully refined
  - Thickening of 2D mesh: $0.81\,\mathrm{mm}$ on both sides (real $0.445\,\mathrm{mm}$)
- Solid: SFC thin-shell solver by F. Cirak
  - Aluminum, J2 plasticity with hardening, rate sensitivity, and thermal softening
  - Mesh: 8577 nodes, 17056 elements
- 64+8 processors 2.2 GHz AMD Opteron, PCI-X 4x Infiniband network, $\sim 4320\,\mathrm{h}$ CPU to $t_{end} = 450\,\mu\mathrm{s}$


$0.032\,\mathrm{ms}$

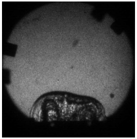
$0.030\,\mathrm{ms}$

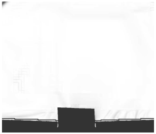
$0.212\,\mathrm{ms}$

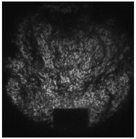
$0.210\,\mathrm{ms}$

Tube with flaps: results

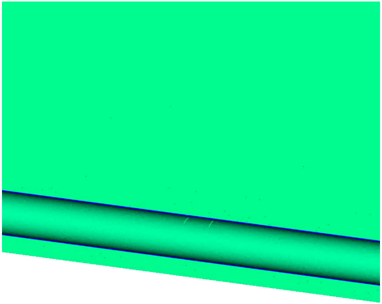

Fluid density and diplacement in y-direction in solid

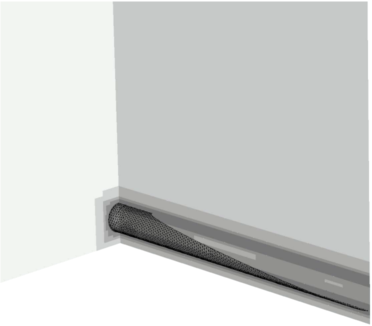

Schlieren plot of fluid density on refinement levels

F. Cirak, RD, and S. P. Mauch (2007). *Computers & Structures*, 85(11-14):1049–1065

UML design of AMROC

- Classical framework approach with generic main program in C++
- Customization / modification in Problem.h include file by derivation from base classes and redefining virtual interface functions
- Predefined, scheme-specific classes (with F77 interfaces) provided for standard simulations
- Standard simulations require only linking to F77 functions for initial and boundary conditions, source terms. No C++ knowledge required
- Interface mimics Clawpack
- Expert usage (algorithm modification, advanced output, etc.) in C++

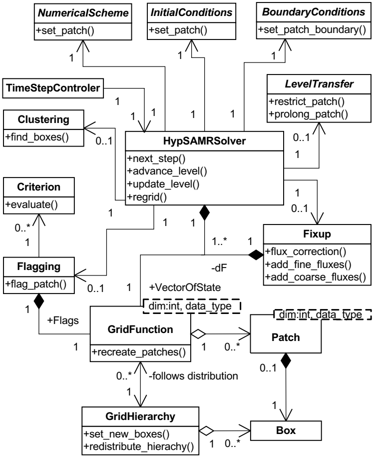

Embedded boundary method / FSI coupling

- Multiple independent EmbeddedBoundaryMethod objects possible
- Specialization of GFM boundary conditions, level set description in scheme-specific F77 interface classes

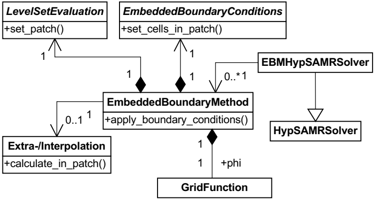

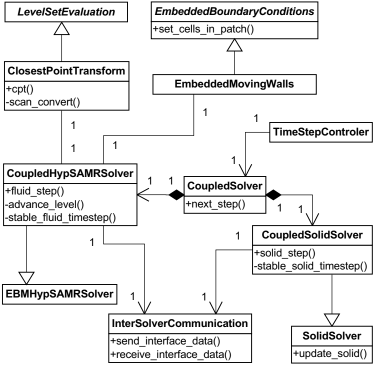

- Coupling algorithm implemented in further derived HypSAMRSolver class
- Level set evaluation always with CPT algorithm
- Parallel communication through efficient non-blocking communication module
- Time step selection for both solvers through CoupledSolver class

The Virtual Test Facility

- Implements all described algorithms
- AMROC V2.0 plus solid mechanics solvers
- Implements explicit SAMR with different finite volume solvers
- Embedded boundary method, FSI coupling
- $\sim 430,000$ lines of code total in C++, C, Fortran-77, Fortran-90
- autoconf / automake environment with support for typical parallel high-performance system
- http://www.cacr.caltech.edu/asc

Performance of AMROC V2.1β

Strong scalability test

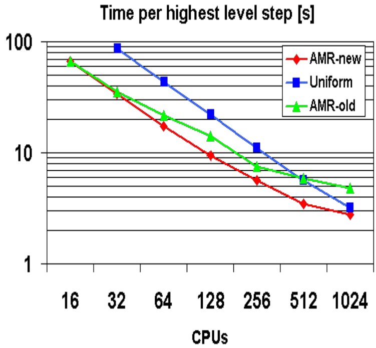

Weak scalability test

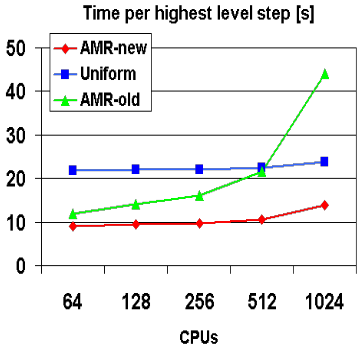

- Spherical blast wave, Euler equations, 3D Wave Propagation Method, test run on IBM BG/P
- AMR base grid with 2 additional levels $r_{1,2} = 2, 4$. 5 time steps on coarsest level
- Weak scalability test on 1024 CPUs: $128 \times 64 \times 64$ base grid, $> 33,500$ Grids, $\sim 61 \cdot 10^6$ cells, uniform $1024 \times 512 \times 512 = 268 \cdot 10^6$ cells
- AMROC V2.1β: major improvements in computation of space-filling curve and metadata organization

Summary

- Developed a generic Cartesian parallel SAMR framework that permits complex geometries and fluid-structure coupling for explicit methods
- Core idea is to combine level-set-based boundary embedding with dynamic mesh adaptation
- Our approach puts the main algorithmic complexity for fluid-structure coupling on the Eulerian fluid side
- It is easy to exchange the solid mechanics solver and the fluid single-patch integrator
- Immediate future directions:
  - Implicit methods for the fluid solver based on adaptive geometric multigrid (prototyped serial Poisson solver so far)
  - Level set methods with dynamic interface between two fluids

References I

[Abgrall and Karni, 2001] Abgrall, R. and Karni, S. (2001). Computations of compressible multifluids. *J. Comput. Phys.*, 169:594–523.

[Arienti et al., 2003] Arienti, M., Hung, P., Morano, E., and Shepherd, J. E. (2003). A level set approach to Eulerian-Lagrangian coupling. *J. Comput. Phys.*, 185:213–251.

[Berger and Colella, 1988] Berger, M. and Colella, P. (1988). Local adaptive mesh refinement for shock hydrodynamics. *J. Comput. Phys.*, 82:64–84.

[Berger and Oliger, 1984] Berger, M. and Oliger, J. (1984). Adaptive mesh refinement for hyperbolic partial differential equations. *J. Comput. Phys.*, 53:484–512.

[Davis, 1988] Davis, S. F. (1988). Simplified second-order Godunov-type methods. *SIAM J. Sci. Stat. Comp.*, 9:445–473.

[Deshpande et al., 2006] Deshpande, V. S., Heaver, A., and Fleck, N. A. (2006). An underwater shock simulator. *Royal Society of London Proceedings Series A*, 462(2067):1021–1041.

[Falcovitz et al., 1997] Falcovitz, J., Alfandary, G., and Hanoch, G. (1997). A two-dimensional conservation laws scheme for compressible flows with moving boundaries. *J. Comput. Phys.*, 138:83–102.

References II

[Fedkiw, 2002] Fedkiw, R. P. (2002). Coupling an Eulerian fluid calculation to a Lagrangian solid calculation with the ghost fluid method. *J. Comput. Phys.*, 175:200–224.

[Giordano et al., 2005] Giordano, J., Jourdan, G., Burtschell, Y., Medale, M., Zeitoun, D. E., and Houas, L. (2005). Shock wave impacts on deforming panel, an application of fluid-structure interaction. *Shock Waves*, 14(1-2):103–110.

[Harten, 1983] Harten, A. (1983). High resolution schemes for hyperbolic conservation laws. *J. Comput. Phys.*, 49:357–393.

[Langseth and LeVeque, 2000] Langseth, J. and LeVeque, R. (2000). A wave propagation method for three dimensional conservation laws. *J. Comput. Phys.*, 165:126–166.

[LeVeque, 1997] LeVeque, R. J. (1997). Wave propagation algorithms for multidimensional hyperbolic systems. *J. Comput. Phys.*, 131(2):327–353.

[Mader, 1979] Mader, C. L. (1979). *Numerical modeling of detonations*. University of California Press, Berkeley and Los Angeles, California.

References III

[Mauch, 2003] Mauch, S. P. (2003). *Efficient Algorithms for Solving Static Hamilton-Jacobi Equations*. PhD thesis, California Institute of Technology.

[Quirk, 1994] Quirk, J. J. (1994). A contribution to the great Riemann solver debate. *Int. J. Numer. Meth. Fluids*, 18:555–574.

[Rendleman et al., 2000] Rendleman, C. A., Beckner, V. E., Lijewski, M., Crutchfield, W., and Bell, J. B. (2000). Parallelization of structured, hierarchical adaptive mesh refinement algorithms. *Computing and Visualization in Science*, 3:147–157.

[Roe, 1981] Roe, P. L. (1981). Approximate Riemann solvers, parameter vectors and difference schemes. *J. Comput. Phys.*, 43:357–372.

[Sanders et al., 1998] Sanders, R., Morano, E., and Druguett, M.-C. (1998). Multidimensional dissipation for upwind schemes: Stability and applications to gas dynamics. *J. Comput. Phys.*, 145:511–537.

[Sethian, 1999] Sethian, J. A. (1999). *Level set methods and fast marching methods*. Cambridge University Press, Cambridge, New York.

[Shyue, 1998] Shyue, K.-M. (1998). An efficient shock-capturing algorithm for compressible multicomponent problems. *J. Comput. Phys.*, 142:208–242.

References IV

[Shyue, 2006] Shyue, K.-M. (2006). A volume-fraction based algorithm for hybrid barotropic and non-barotropic two-fluid flow problems. *Shock Waves*, 15:407–423.

[Specht, 2000] Specht, U. (2000). *Numerische Simulation mechanischer Wellen an Fluid-Festkörper-Mediengrenzen*. Number 398 in VDI Reihe 7. VDU Verlag, Düsseldorf.

[Toro, 1999] Toro, E. F. (1999). *Riemann solvers and numerical methods for fluid dynamics*. Springer-Verlag, Berlin, Heidelberg, 2nd edition.

[Toro et al., 1994] Toro, E. F., Spruce, M., and Speares, W. (1994). Restoration of the contact surface in the HLL-Riemann solver. *Shock Waves*, 4:25–34.

[Westbrook, 1982] Westbrook, C. K. (1982). Chemical kinetics of hydrocarbon oxidation in gaseous detonations. *Combust. Flame*, 46:191–210.